THE ASTROPHYSICAL JOURNAL, 472:665–672, 1996 December 1

THREE MICRON HYDROCARBON AND METHANOL ABSORPTION IN TAURUS

J. E. CHIAR
Rensselaer Polytechnic Institute, Department of Physics, Applied Physics and Astronomy, Troy, NY 12180
A. J. ADAMSON
Centre for Astrophysics, University of Central Lancashire, Corporation Street, Preston PR1 2HE, England, U.K.
AND
D. C. B. WHITTET
Rensselaer Polytechnic Institute, Department of Physics, Applied Physics and Astronomy, Troy, NY 12180
Received 1996 February 26; accepted 1996 June 14

ABSTRACT

The 3.3–4.0 μm spectral region contains the fundamental C-H stretching vibrations of alcohols and aliphatic hydrocarbons and provides a powerful method of characterizing the organic component of interstellar ices. Observations of sources in and behind the Taurus dark cloud are presented. We detect the 3.47 μm hydrocarbon feature toward Elias 16 (field star) and HL Tau (T Tauri star). Elias 16 provides the first detection of the 3.47 μm feature in the quiescent cloud medium. Our results are consistent with a location for the 3.47 μm absorber in the grain mantle material rather than the core. The 3.54 μm methanol (CH_3OH) feature is not detected in any of the sources to a limit of $\tau_{3.54}/A_V < 0.0009$, and CH_3OH therefore has an abundance relative to H_2O, which is likely to be less than 5%. This result sets limits on models for mantle evolution which involve processing of CH_3OH-rich ices to form more complex organic species in regions of active star formation.

Subject headings: dust, extinction — infrared: ISM: lines and bands — ISM: molecules

1. INTRODUCTION

Carbonaecous material in the interstellar medium (ISM) takes many forms. These might include graphite (a common constituent of many grain models; see Mathis, Rumpl, & Nordsieck 1977), aliphatic hydrocarbons (Adamson, Whittet, & Duley 1990; Pendleton et al. 1994), polycyclic hydrocarbons (Puget 1989), simple alcohols and other organic molecules in dark clouds (Schutte et al. 1995; Allamandola et al. 1992; Skinner et al. 1992), SiC (seen in emission in carbon stars but currently of controversial abundance in the ISM; Whittet, Duley, & Martin 1990), and possibly microscopic diamonds (Allamandola et al. 1992). Evolution of the chemical properties of such material as it cycles through diffuse and dense clouds is a subject of increasing interest (see Duley & Williams 1995). However, modeling the evolution of carbonaceous matter is complicated by its ability to take on such a wide variety of forms. Observations of the dominant forms as a function of interstellar environment may help to determine the evolutionary paths taken by these materials.

Spectroscopy between 3.3 and 4.0 μm is crucial to defining the nature of organic material since fundamental C-H stretching vibrations occur in this spectral region, at characteristic wavelengths which reflect the form of the carbon bonding. The C-H stretching vibration around 3.4 μm, dominant in the diffuse ISM, has been well observed and is known to be associated with saturated aliphatic hydrocarbons (Butchart et al. 1986; Adamson, Whittet, & Duley 1991; Sandford et al. 1991; Pendleton et al. 1994). Three micron spectroscopy of dust in dark clouds has revealed a number of very weak features, appearing as substructure in the long-wavelength wing of the H_2O-ice band. Their origins are at present only weakly constrained. Allamandola et al. (1992) detected a band at 3.47 μm in luminous protostellar objects, which they attributed to sp^3-bonded hydrocarbon material (the carbon atoms are bonded in a "diamond-like" configuration). The identification of the 3.47 μm feature with C-H bonds on sp^3-bonded carbon atoms is uncertain and is based mainly on abundance ratios (of primary, secondary, and tertiary carbons) calculated from one high S/N spectrum (Allamandola et al. 1992). However, it remains a plausible candidate for the absorber (see Brooke, Sellgren, & Smith 1996). Sellgren, Smith, & Brooke (1994) also detected a similar band in Mon R2 IRS 3. Significantly, none of the above absorption features was detected by Sellgren et al. in the line of sight to Elias 16 (a background giant sampling the margins of the dense core TMC-1).

Solid methanol (CH_3OH) is of controversial abundance in dark clouds, although its presence in lines of sight towards a few protostars is fairly well established. It absorbs at 3.54 μm in the lines of sight to W33A, NGC 7538 IRS 9 (Grim et al. 1991; Allamandola et al. 1992), and GL 2136 (Schutte et al. 1995) and produces narrow 8.9 and 9.7 μm bands (due to the CH_3 rock and CO stretch, respectively) in GL 2136 (Skinner et al. 1992). A feature coincident with the C-H deformation mode in CH_3OH at 6.85 μm is also detected in several protostellar sources including W33A and NGC 7538 IRS 9. However, the 3.54 μm feature is not detected towards Mon R2 IRS 3 or Elias 16 (Sellgren et al. 1994). If CH_3OH is indeed only present towards very luminous protostars, it is important to understand why. Recent chemical models (see Caselli, Hasegawa, & Herbst 1994; Hasegawa & Herbst 1993) produce solid methanol through hydrogenation reactions of CO in grain mantles, consistent with the suggestion by Skinner et al. that CH_3OH is not mixed with H_2O-ice (since spatial segregation of solid CO and H_2O in grain mantles is well established; see Kerr, Adamson, & Whittet 1993). In these models, the rate of CO hydrogenation has a controlling influence on the abundance of CO; at a given evolutionary stage, therefore, the CH_3OH/CO ratio would be expected to be an indicator of

TABLE 1

PROGRAM STARS AND OBSERVATIONAL PARAMETERS

Source	Identification[a]	Spectral Type[a]	Comparison Star and Spectral Type
Elias 3	Field star	K2 III	BS 1529 (K2 III)
Elias 13	Field star	K2 III	BS 1529 (K2 III)
Elias 15	Field star	M2 III	BS 1280 (K5 III)
Elias 16	Field star	K1 III	BS 1529 (K2 III)
Elias 18	Embedded	B5	BS 1319 (F5 V)
Tamura 8.....	Field star	K5 III	BS 1280 (K5 III)
HL Tau.....	T Tauri	K7e	BS 1319 (F5 V)

[a] Identification and spectral type for Tamura 8 from Tamura et al. 1987 and Whittet et al. 1988; HL Tau from Cohen & Kuhi 1979 and Cohen 1983; all others from Elias 1978.

this rate. However, comparisons between models and observations have shown that CH_3OH is most likely mixed with at least some H_2O in the mantles (Allamandola et al. 1992; Schutte et al. 1996). Energetic processing of CH_3OH-containing ices by UV irradiation produces organic residues (see review by Schutte 1996 and references therein) and is thus thought to be a key molecule in the production of organic compounds in interstellar and cometary ices (Bernstein et al. 1995).

Data presented in this paper place limits on the abundance of simple hydrocarbons and solid-phase methanol in the lines of sight to less luminous sources in and behind the Taurus dark cloud. They are compared to the abundances of other solid phase molecules (H_2O and CO) in the same lines of sight. We address the following questions: (1) does the feature at 3.47 μm first detected by Allamandola et al. (1992) arise in the icy mantle or the refractory component of the grains? (2) Is CH_3OH a widespread component of protostellar and/or molecular cloud ices? The observations, obtained with CGS4 on UKIRT, and data reduction are described in § 2. Section 3 presents detections of the 3.47 μm feature and discusses the nature of its carrier. In § 4 we discuss the significance of the methanol nondetections and its abundance relative to H_2O. In § 5 we summarize our results.

2. OBSERVATIONS AND DATA REDUCTION

Two embedded objects and five field stars in and behind the Taurus dark cloud were observed on 1993 November 13 and 14 using CGS4 on the United Kingdom Infrared Telescope (UKIRT) at Mauna Kea in Hawaii. The 75 lines mm^{-1} grating was used with the 58 × 62 pixel detector array giving wavelength coverage of 0.4 μm with an unsmoothed spectral resolution of 0.003 μm. Secondary chopping was carried out with a throw of 24″.6 north-south, and nodding by the same distance in the same direction was also performed to remove second-order background gradients. Weather conditions during the majority of the observations were good, but observations on the second night (of Elias 18, HL Tau, and Tamura 8) were affected by cloud and variable transparency. The spectra were oversampled by stepping the detector array in four steps over two resolution elements, and transparency variations between array settings therefore produced periodic ripples in some spectra; these were successfully removed using the STARLINK FIGARO IRFLAT routine. Error bars in the spectra presented here are purely statistical in the sense that each spectrum is the result of a number of separate observations; error bars were determined by first normalizing the individual observations to the mean and then determining the standard error of the counts at each wavelength. This procedure avoids the spuriously large error bars which would be present in cases of transparency variations if the individual observations were not first normalized together but is not intended to give an indication of flux calibration precision.

Cancellation of telluric absorption was achieved by ratioing with standard stars observed at similar air mass. The comparison stars are listed in Table 1. The wavelength scale for all objects was calibrated using an argon lamp and is accurate to within 0.001 μm.

The derived optical depth and column density of absorbing material in these lines of sight are crucially dependent upon the choice of continuum for such weak absorption features: this is hindered by the presence of strong telluric CH_4 absorption on the short-wavelength side of the bands. Continua in the region between 3.31–3.72 μm were fit using the STARLINK FIGARO ABLINE routine and are shown in Figure 1. Third-degree polynomials were used so as not to reduce the strength of a feature as narrow as the methanol band. We note that the exact choice of absorption-free sections of the spectrum can significantly affect the results. A good illustration of these difficulties may be found in the spectrum of S140 IRS 1 presented by Allamandola et al. (1992), where the continuum around 3.3 μm is hardly constrained by the data.

Our spectrum of Elias 16 shows absorption due to the P branch of photospheric OH (Beer et al. 1972), as does that presented by Sellgren et al. (1994). In both cases the standard was closely matched in spectral type to that inferred for Elias 16. The residual absorption lines were removed before fitting the continuum. Figure 2 shows the optical depth spectra for Elias 16 and HL Tau. Figures 3*a*–3*e* shows the optical depth spectra for the remainder of the sources and Figures 3*f*–3*g* show the optical depth spectra of Elias 16 and HL Tau after removal of the 3.47 μm absorption feature (see below).

3. THE 3.47 μm FEATURE

To date, only YSOs, embedded deep in their parental clouds, have been shown to exhibit the 3.47 μm absorption feature. Figure 2*a* shows the detection of this band in the highly reddened field star Elias 16 ($A_V \sim 22.3$; Elias 1978; Smith, Sellgren, & Brooke 1993); this is the first definitive observation of this feature in the line of sight through the quiescent dark cloud medium. We have also detected this feature in HL Tau (Fig. 2*b*), a young T Tauri star with $A_V > 22$ (Stapelfeldt et al. 1995).[1] To quantify the optical depth of the 3.47 μm feature, we fit a Gaussian to the profile allowing the height, width, and central wavelength to vary. For Elias 16, this procedure yields a central wavelength of $\lambda_0 = 3.471$ μm, an optical depth of $\tau = 0.032 \pm 0.002$, and FWHM $= 60 \pm 6$ cm^{-1}. We believe this is a definitive detection, just below the level of the upper limit derived from CGAS data by Sellgren et al. (1994). A Gaussian fit to HL Tau yields $\lambda_0 = 3.455$ μm, $\tau = 0.035 \pm 0.005$, and FWHM $= 50 \pm 5$ cm^{-1}. The fitted Gaussians for Elias 16 and HL Tau are shown in Figures 2*a* and 2*b*, respectively.

[1] Stapelfeldt et al. recalculate the visual extinction of HL Tau based on new optical photometry from WPFC2 on HST. This new calculation has taken into account reflected light from the object leading to a photospheric luminosity and A_V greater than previous estimates.

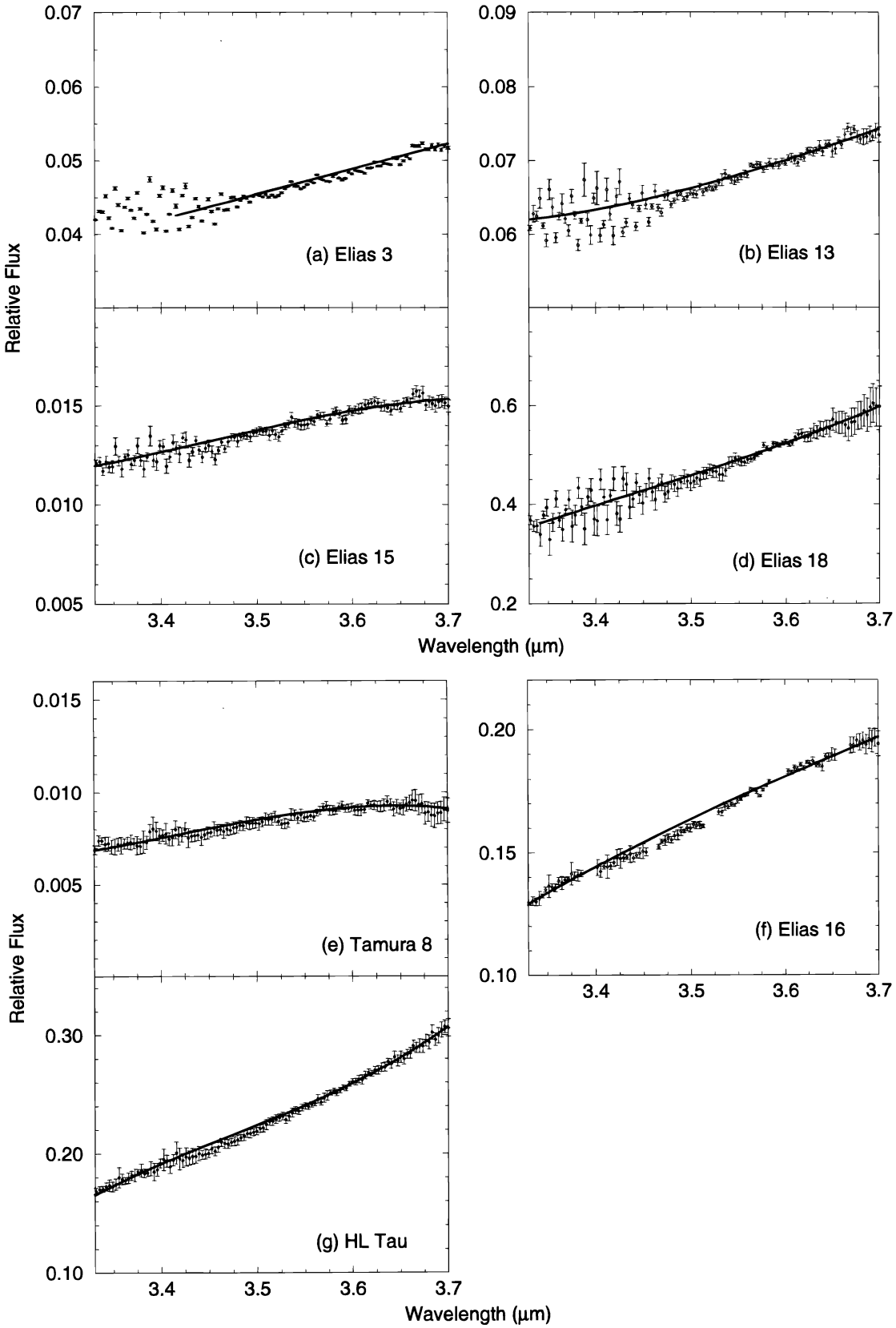

FIG. 1.—Rectified spectra with local fitted continua: (*a*) Elias 3, (*b*) Elias 13, (*c*) Elias 15. (*d*) Elias 18, (*e*) Tamura 8, (*f*) Elias 16, (*g*) HL Tau

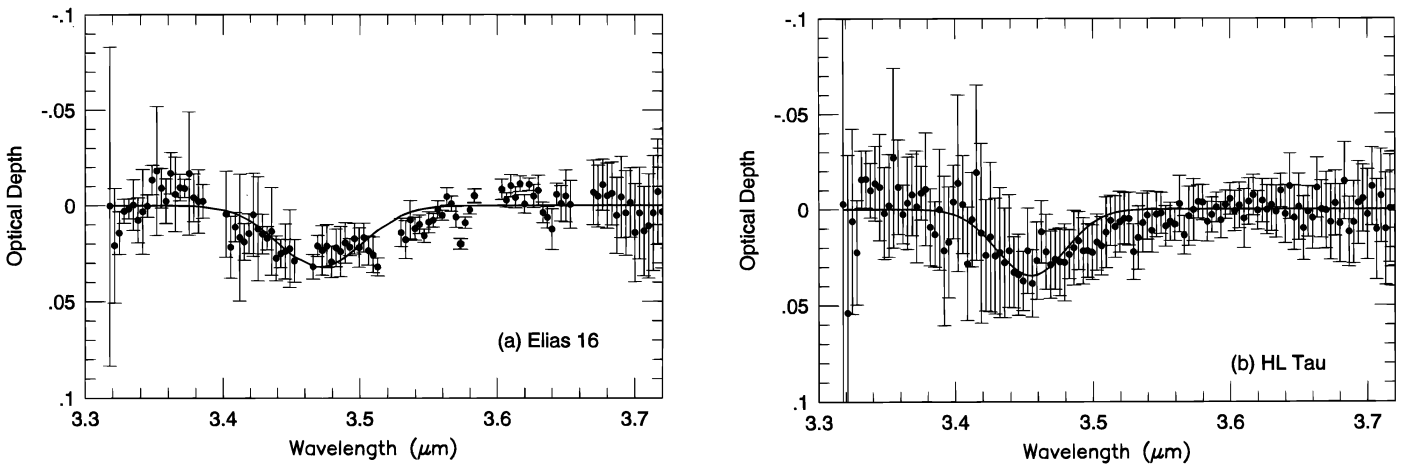

FIG. 2.—3.47 μm absorption feature towards (*a*) Elias 16 and (*b*) HL Tau. The solid line is the fitted Gaussian with parameters given in Table 2.

This feature is not detected in the spectra of the other program stars (Elias 3, 13, 15, 18, and Tamura 8)[2]. We compute limiting values for these sources using a χ^2 statistic to determine the 1 σ allowable optical depth using a Gaussian with FWHM = 80 cm^{-1} and central wavelength, λ_0 = 3.47 μm. Table 2 lists these optical depths for all sources.

There is growing evidence to suggest that the molecule responsible for the 3.47 μm feature is associated with the mantle rather than the core material (Brooke et al. 1996). The variation of its strength relative to that of the 3.54 μm CH_3OH feature has been used to suggest that it is due to refractory material (Allamandola et al. 1992). However, it is not clear that all mantled grains contain CH_3OH ice as some lines of sight with 3.1 μm H_2O-ice absorption, do not exhibit the 3.54 μm CH_3OH band (see Allamandola et al. 1992; Sellgren et l. 1994; Brooke et al. 1996). Brooke et al. (1996) have shown that there is little correlation between the 3.47 μm feature and the 9.7 μm silicate feature. Adding Elias 16, HL Tau, and HH100-IR (Graham 1996, private communication; Whittet et al. 1996) to the plot of $\tau_{3.47}$ versus $\tau_{9.7}$ does not improve the correlation coefficient which we calculate to be ~0.57. However, Whittet et al. (1988) have shown that $\tau_{9.7}$ does not correlate very well against A_V for Taurus sources, and thus a correlation of $\tau_{3.47}$ and $\tau_{9.7}$ was likely to be poor. The optical depths of the 3.47 μm feature and 3.1 μm H_2O-ice feature are strongly correlated (Brooke et al. 1996). We plot these data in Figure 4. A least-squares fit (excluding limiting values) gives $\tau_{3.47} = (0.03 \pm 0.01)\tau_{3.1} - (0.00 \pm 0.01)$, in agreement with the Brooke et al. (1996) result. This correlation ($r \sim 0.90$) supports the conclusion that the 3.47 μm feature is due to some part of the mantle material. The correlation goes through the origin, suggesting that the H_2O ice and the 3.47 μm carrier co-exist in the grain mantle and ruling out the idea that the carrier of the 3.47 μm feature exists in the core (or an inner mantle layer) before the H_2O ice forms.

Additional support is given by the difference in structure between the 3.47 μm molecular cloud feature and the 3.4 μm diffuse ISM feature attributed to $-CH_2-$ and $-CH_3$ groups of aliphatic hydrocarbons (Butchart et al. 1986; Adamson et al. 1991; Sandford et al. 1991; Pendleton et al. 1994). The diffuse ISM feature is known to be spatially correlated with silicates (Sandford, Pendleton, & Allamandola 1995), whereas the molecular cloud feature is not. Figure 5 shows the spectrum of the Galactic center source IRS 6E (Pendleton et al. 1994) and Elias 16 scaled to the depth of the 3.47 μm feature in Elias 16. The diffuse ISM feature has definite substructure due to $-CH_2-$ and $-CH_3$ groups which is not seen in the dense cloud dust (Pendleton 1993; 1994). The feature near 3.4 μm seen in GRC IRS 6E is apparently missing in dense cloud spectra such as that of Elias 16. Greenberg et al. (1995) have compared the spectrum of IRS 6E with simple ices (containing H_2O, CO, NH_3, CH_4, CH_3OH, and C_2H_2) processed by solar UV radiation. These irradiated samples mimic the cyclic UV processing of interstellar dust as it cycles between the molecular and diffuse cloud environments. Given the relatively short cycling time between the diffuse and dense cloud regions, we would expect to see the 3.4 μm aliphatic hydrocarbon features in both environments. Their apparent absence in the dense cloud dust could change our view of interstellar grain evolution and our understanding of the origin of the organic component in the ISM. However, a recent study (Duley & Williams 1995) suggests that the physical and chemical properties of carbonaceous dust may

[2] We do not preclude the presence of broad absorption centered at ~3.47 μm, with $\tau < 0.03$, in Tamura 8, but the S/N of this spectrum is too low to make a definite identification.

TABLE 2

TAURUS SOURCES: RESULTS OF χ^2 STATISTIC AND GAUSSIAN FITS

Source	$\tau_{3.54}$	$\tau_{3.47}$[a]	FWHM$_{3.47}$[b] (cm^{-1})
Elias 3	<0.01	...	...
Elias 13	<0.01	<0.02	80
Elias 15	<0.02	<0.03	80
Elias 16	<0.02	0.032 ± 0.002	60
Elias 18	<0.02	<0.03	80
Tamura 8.....	<0.05	<0.03	80
HL Tau.....	<0.02	0.035 ± 0.005	50

[a] Limiting values are from χ^2 statistics as described in text. Due to insufficient cancellation of telluric methane, a limiting value for Elias 3 could not be calculated.

[b] FWHM = 80 cm^{-1} is the value chosen to best represent an average FWHM of sources observed to date. Other values are from Gaussian fits to the feature.

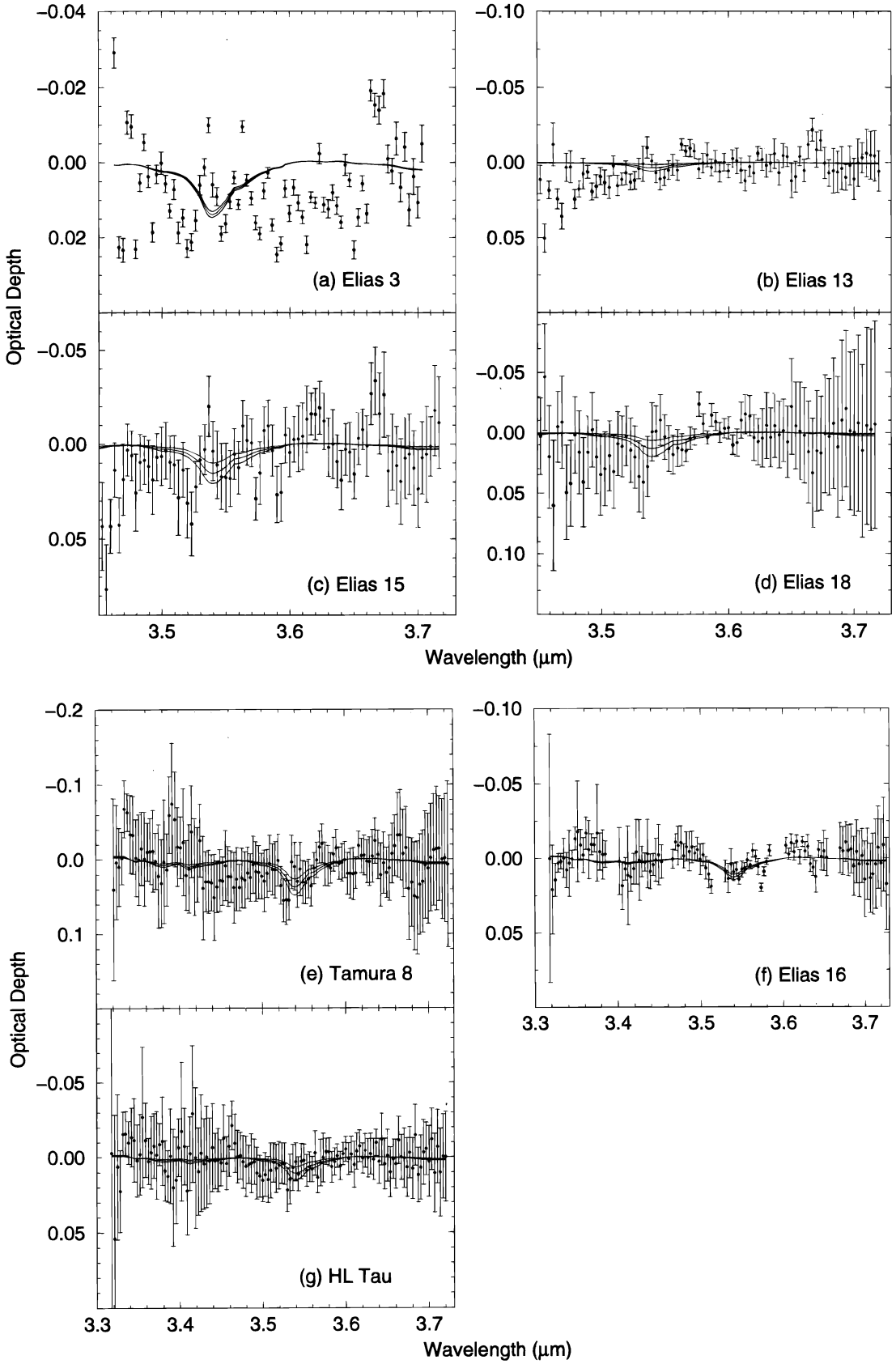

FIG. 3.—Optical depth spectra with methanol lab data (Allamandola et al. 1992): (*a*) Elias 3, (*b*) Elias 13, (*c*) Elias 15, (*d*) Elias 18, (*e*) Tamura 8, (*f*) Elias 16, (*g*) HL Tau. The 3.47 μm feature has been subtracted in Elias 16 and HL Tau. The middle solid line is the best estimate for the depth of the methanol feature. The lower and upper lines signify $\delta\chi = \pm 1$ showing the allowable depth of the feature within a 68% confidence limit.

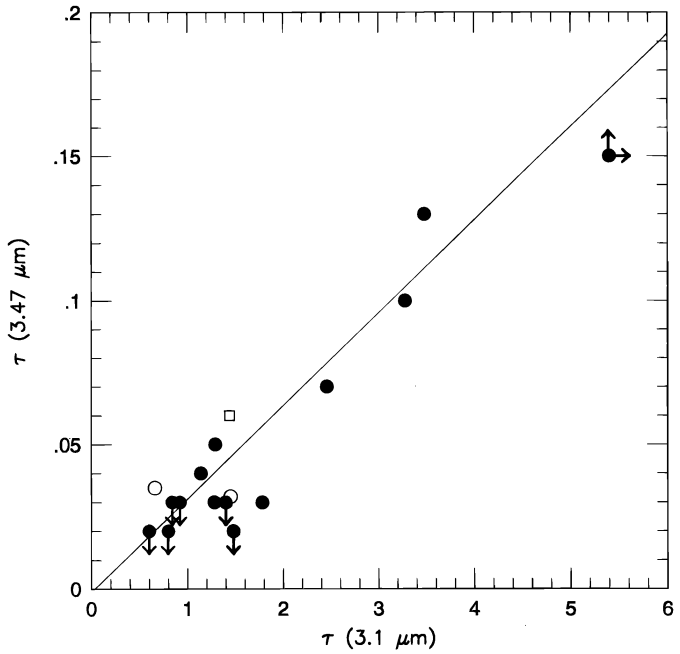

FIG. 4.—Plot of $\tau_{3.47}$ vs. $\tau_{3.1}$: solid circles are from data tabulated in Brooke et al. (1996); open circles are Elias 16 and HL Tau, open square is HH100-IR (Graham 1996, private communication). The solid line represents the least-squares fit to the points excluding limiting values.

be significantly altered during its lifetime by heating and exposure to UV radiation. It is possible that the carbonaceous dust changes form as it cycles through the dense and diffuse ISM, and thus we would not expect to see the same material in both environments.

4. THE 3.54 μm METHANOL FEATURE

We do not detect the 3.54 μm CH_3OH feature toward either the field stars or embedded objects in this study. The optical depth spectra are shown in Figure 3. In the cases of Elias 16 and HL Tau the 3.47 μm feature was removed by fitting a Gaussian to the profile and subtracting it before limiting values for $\tau_{3.54}$ were calculated. This allows for the fact that absorption at 3.54 μm for these objects is at least partially due to the 3.47 μm feature. The resulting optical depth spectra of all sources were fitted with the CH_3OH (10 K) lab spectrum from Allamandola et al. (1992, their Fig. 5) using a χ^2 statistic to place a quantitative limit on the optical depth of the band. The optical depth spectra and fitting results are shown in Figure 3. In each case, we show the best estimate for the optical depth (*middle curve*) and lower and upper 68% confidence limits. Although the feature is formally detected in these fits, we conservatively adopt the lower curve as an upper limit for the optical depth of the methanol feature. The corresponding column densities are calculated using the equation

$$N = \frac{\Delta v \tau}{A}, \quad (1)$$

where τ in this case is the adopted optical depth limit and $\Delta v = 30$ cm^{-1} (Allamandola et al. 1992). The integrated absorption strength, $A = 7.5 \times 10^{18}$ cm molecule^{-1} for H_2O:CH_3OH:CO:NH_3 ice (100:10:1:1) at 10 K (Hudgins et al. 1993). Comparisons of observational data with laboratory spectra have shown that methanol is most likely embedded in an H_2O-ice matrix, rather than existing in pure form (Allamandola et al. 1992; Schutte et al. 1995). The absorption strength of the methanol band is a function of the relative amounts of CH_3OH and H_2O (e.g., a CH_3OH:H_2O ratio of 2:1 instead of 10:1 results in a 20% increase in A and thus a 20% decrease in the column density estimate). Limiting values for the optical depths and column densities are listed in Tables 2 and 3, respectively. To make valid comparisons, column densities for sources in the literature are recalculated using the same A value and are tabulated in Table 3.

The spectra presented in Figure 3 appears to lack a detectable solid methanol feature. However, the limits placed on the abundance of CH_3OH are insufficiently stringent to conclude that this molecule is grossly underabundant in the Taurus cloud compared with other lines of sight for which data exist. To data, only three sources (all YSOs) have 3.54 μm methanol detections: NGC 7538 IRS 9. W33A, and GL 2136. Of these, W33A has a limiting H_2O-ice measurement (due to an optically thick H_2O-ice absorption feature; Willner et al. 1982), so $N(CH_3OH)/N(H_2O)$ is also a limiting value. The methanol abundance toward NGC 7538 IRS 9 and GL 2136 is observed to be no more than ~5% of the H_2O-ice abundance (see Table 3). This is in agreement with models of Shalabiea & Greenberg (1994) for UV photoproduction of CH_3OH from a mixture of H_2CO and H_2O, which show that its abundance can range from less than 1% to 5% of the H_2O-ice abundance. We use these results to predict the strength of the CH_3OH feature in the Taurus sources, while noting that the H_2O:CH_3OH ratio may change with environment (see below). If the methanol abundance in the Taurus cloud were ~5%, the deepest features, with $\tau_{3.54} \sim 0.03$, would be expected toward the field stars Elias 16 and Tamura 8. An optical depth of 0.03 is 3 σ above the rms in the Elias 16 spectrum and should, in principle, be detectable. The profile fitting described above implies $\tau_{3.54} < 0.02$ in Elias 16, however, suggesting that this line of sight is at least somewhat deficient in CH_3OH. However, it should be borne in mind that the spectrum of Elias 16 is complicated by OH absorption lines and broad absorption at 3.47 μm,

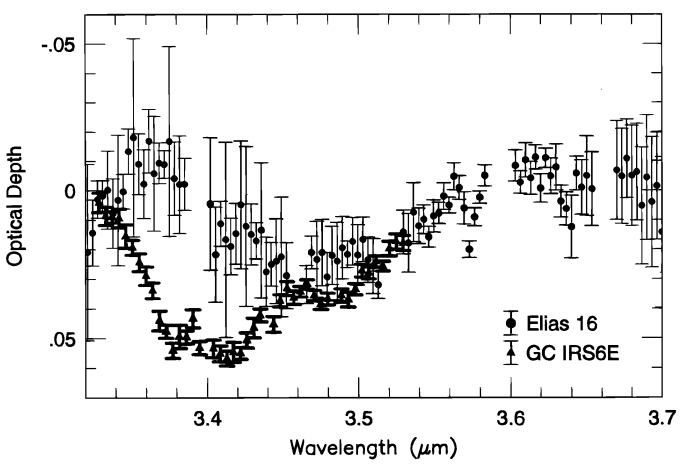

FIG. 5.—3.4 μm absorption feature towards the Galactic center source GC IRS 6E (from Pendleton et al. 1994; *triangles*) and Elias 16 (*circles*) scaled to the depth of the 3.47 μm feature in Elias 16.

TABLE 3

COLUMN DENSITY COMPARISONS

Source	$N(CH_3OH)$ ($\times 10^{17}$ cm^{-2})	Reference	$\frac{N(CO)}{N(H_2O)}$	$\frac{N(CH_3OH)}{N(H_2O)}$	Reference[a]	$\frac{N(CH_3OH)}{N(CO)}$	Reference[b]
Taurus Sources							
Elias 3	<0.56	1	0.20	<0.06	2	<0.31	3
Elias 13	<0.24	1	0.09	<0.02	2	<0.26	3
Elias 15	<0.84	1	0.29	<0.05	2	<0.18	4
Elias 16	<0.72	1	0.25	<0.03	2	<0.11	3
Elias 18	<0.80	1	0.16	<0.06	2	<0.36	3
Tamura 8	<1.92	1	0.23	<0.08	2	<0.35	3
HL Tau	<0.72	1	0.04	<0.07	2	<1.80	4
Other Protostellar Sources							
W33A	20.8	5	<0.04	<0.23	5	5.33	13
NGC 7538/IRS 9	3.2	10	0.14	0.05	5	0.95	13
GL 2136	2.0	12	0.04	0.04	12	1.11	6, 12
S140/IRS 1	<2.0	5	...	<0.10	9	...	...
GL 961E	<1.6	10	0.08	<0.04	8	<0.46	11
Mon R2/IRS 3	<0.9	7	<0.03	<0.05	8	<1.80	11
W3/IRS 5	<0.8	10	0.03	<0.01	8	<3.23	13

[a] Reference for H_2O-ice column density.

[b] Reference for CO column density.

REFERENCES.—1. This work. 2. Estimated from spectra in Whittet et al. 1988. 3. Chiar et al. 1995. 4. Whittet et al. 1989. 5. Allamandola et al. 1992. 6. Skinner et al. 1992. 7. Sellgren et al. 1994. 8. Smith et al. 1989. 9. Willner et al. 1982. 10. Brooke et al. 1996. 11. Geballe 1986. 12. Schutte et al. 1996. 13. Tielens et al. 1991.

leading to a possible underestimate of the 3.54 μm feature. The limiting value derived for Tamura 8 is close to the expected strength of the feature, but the low signal-to-noise ratio of the spectrum and a spurious feature at 3.53 μm (Fig. 3*e*) precludes a definitive detection. An optical depth of $\tau_{3.54} \sim 0.01$ is expected for Elias 3, 13 and HL Tau and $\tau_{3.54} \sim 0.02$ is expected for Elias 15 and 18, comparable to their rms noise.

If methanol is indeed underabundant in the quiescent cloud material represented by Elias 16, one possible explanation is inefficient hydrogenation of CO into CH_3OH. The relatively high observed $N(CO)/N(H_2O)$ ratio for, e.g., Elias 16 compared with NGC 7538 IRS 9 and GL 2136 is consistent with such an interpretation. Caselli et al. (1994) argue that surface CO hydrogenation must be inefficient to maintain the high observed abundance of CO in the mantles. This could either reflect selective desorption of hydrogen following cosmic ray grain heating (Hasegawa & Herbst 1993) or the fact that low-temperature hydrogen atom additions to CO ice is an inefficient way to form CH_3OH, as seen in the laboratory (Hiraoka et al. 1994). Thus, it is likely that energetic processing is necessary in order to overcome the reaction barrier to produce methanol by hydrogenation of CO.

Bernstein et al. (1995) propose that methanol is a key molecule in the production of organic compounds in interstellar and cometary ices. Their laboratory experiments on photolysis of ice analogs initially composed of H_2O, CH_3OH, CO, and NH_3 yield a range of more complex organic molecules, largely at the expense of CH_3OH as the primary carbon source. Prominent amongst the products are CN-bearing molecules (formed by photolysis of CH_3OH and NH_3) which might explain the "XCN" feature observed at 4.62 μm in W33A, NGC 7538 IRS 9, and other YSOs (Tegler et al. 1995, and references therein). In the Taurus cloud, XCN is weakly present towards Elias 18 but absent towards Elias 16 (Tegler et al.). However, the laboratory analogs presented by Bernstein et al. have an initial $CH_3OH:H_2O$ ratio of 1:2, a factor of $\sim$10 higher than has been observed in any source. This might still be a reasonable starting point for YSOs such as NGC 7538 IRS 9, where it can be argued that much of the CH_3OH has already been processed to CN-bearing molecules and other organics. However, toward Elias 16, we are presumably observing more pristine ices in an environment where the only significant source of energetic processing comes from cosmic rays; it is therefore difficult to argue that the CH_3OH abundance is low becuse much of it has already been processed to more complex substances. We conclude that our upper limit for Elias 16 and other field stars in Taurus may place useful constraints on models for the chemical evolution of mantles.

5. CONCLUSIONS

We have presented spectra of the 3 μm H_2O-ice long-wavelength wing for sources in and behind the Taurus dark cloud in an effort to (1) identify the carrier of the 3.47 μm feature, and (2) place limits on the solid-state methanol abundance in dark clouds. We have produced the first detection of the 3.47 μm feature towards a field star (Elias 16) showing that a protostellar environment is not a prerequisite for appearance of the feature. The fact that its strength is similar in Elias 16 to that in YSOs with similar $\tau_{3.1}$ suggests that it is a universal molecular cloud feature; furthermore, the close correlation between $\tau_{3.1}$ and $\tau_{3.47}$ strongly supports the idea that its carrier resides in the grain mantles.

Comparison of the 3.47 μm dense cloud feature and the 3.4 μm diffuse cloud feature shows distinct differences in their structure. These features appear to be due to different forms of hydrocarbon material. Although the dust cycling time between the diffuse and dense clouds is relatively short, it has been suggested that carbonaceous material is processed as it is exposed to heating and UV radiation. The

differences between the features is suggestive that the carriers have indeed been altered.

We did not detect the 3.54 μm solid methanol feature toward either field stars or embedded objects. Our upper limits on the abundance of CH_3OH (3%–8%) are of the same order as previous *detections* toward deeply embedded YSOs in other clouds. This is perhaps surprising if CH_3OH is a "primary" ice, abundant in relatively pristine condensates and subsequently processed to complex molecules when stars are formed within the cloud. However, methanol is also underabundant in the *gas phase* in Taurus (Friberg et al. 1988) relative to more active star-forming regions (e.g., Sutton et al. 1995). This implies that the difference in local energy density (i.e., luminosity) is a factor and supports the idea that energetic processing is necessary to produce methanol.

We thank the staff of UKIRT for their assistance during the run and John Graham for sending us a spectrum of HH100-IR prior to publication. We also thank the anonymous referee for helpful comments. J. E. C. acknowledges support from the Department of Education. D. C. B. W. and J. E. C. acknowledge support from NASA grants NAGW 3144 (Long-Term Space Astrophysics) and NAGW 4039 (Infrared Space Observatory). A. J. A. is supported partly by the University of Central Lancashire and partly by the U.K. Starlink project. D. C. B. W. and A. J. A. also acknowledge support from NATO.

REFERENCES

Adamson, A. J., Whittet, D. C. B., & Duley, W. W. 1990, MNRAS, 243, 400
———. 1991, MNRAS, 252, 234
Allamandola, L. J., Sandford, S. A., Tielens, A. G. G. M., & Herbst, T. M. 1992, ApJ, 399, 134
Beer, R., Hutchison, R. B., Norton, R. H., & Lambert, D. L. 1972, ApJ, 172, 89
Bernstein, M. P., Sandford, S. A., Allamandola, L. J., Chang, S., & Scharberg, M. A. 1995, ApJ, 454, 327
Brooke, T. Y., Sellgren, K., & Smith, R. G. 1996, ApJ, 459, 209
Butchart, I., McFadzean, A. D., Whittet, D. C. B., Geballe, T. R., & Greenberg, J. M. 1986, A&A, 154, 5L
Caselli, P., Hasegawa, T. I., & Herbst, E. 1994, ApJ, 421, 206
Chiar, J. E., Adamson, A. J., Kerr, T. H., & Whittet, D. C. B. 1995, ApJ, 455, 234
Cohen, M. 1983, ApJ, 270, L69
Cohen, M., & Kuhi, L. V. 1979, ApJS, 41, 743
Duley, W. W., & Williams, D. A. 1995, MNRAS, 272, 442
Elias, J. H. 1978, ApJ, 224, 857
Friberg, P., Madden, S. C., Hjalmarson, Å., & Irvine, W. M. 1988, A&A, 195, 281
Geballe, T. R. 1986, A&A, 162, 248
Graham, J. A. 1996, private communication
Greenberg, J. M., Li, A., Mendoza-Gomez, C. X., Schutte, W. A., Gerakines, P. A., & De Groot, M. 1995, ApJ, 455, L177
Grim, R. J. A., Baas, F., Greenberg, J. M., Geballe, T. R., & Schutte, W. 1991, A&A, 243, 473
Hasegawa, T. I., & Herbst, E. 1993, MNRAS, 261, 83
Hiraoka, K., Ohashi, N., Kihara, Y., Yamamoto, K., Sato, T., & Yamashita, A. 1944, Chem. Phys. Lett., 229, 408
Hudgins, D. M., Sandford, S. A., Allamandola, L. J., & Tielens, A. G. G. M. 1993, ApJS, 86, 713
Kerr, T. H., Adamson, A. J., & Whittet, D. C. B. 1993, MNRAS, 262, 1047
Mathis, J. S., Rumpl, W., & Nordsieck, K. H. 1977, ApJ, 217, 425
Pendleton, Y. J. 1993, in ASP Conf. Ser. 41, Astronomical IR Spectroscopy: Future Observational Directions, ed. S. Kwok (San Francisco: ASP), 171
Pendleton, Y. J. 1994, in ASP Conf. Ser. 58, The First Symposium on the Infrared Cirrus and Diffuse Interstellar Clouds, ed. R. M. Cutri & W. B. Latter (San Francisco: ASP), 255
Pendleton, Y. J., Sandford, S. A., Allamandola, L. J., Tielens, A. G. G. M., & Sellgren, K. 1994, ApJ, 437, 683
Puget, J. L. 1989, ARA&A, 27, 161
Sandford, S. A., Allamandola, L. J., Tielens, A. G. G. M., Sellgren, K., Tapia, M., & Pendleton, Y. 1991, ApJ, 371, 607
Sandford, S. A., Pendleton, Y. J., & Allamandola, L. J. 1995, ApJ, 440, 697
Schutte, W. A. 1996, in The Cosmic Dust Connection, ed. J. M. Greenberg (Dordrecht: Kluwer), in press
Schutte, W. A., Gerakines, P. A., Geballe, T. R., van Dishoeck, E. F., & Greenberg, J. M. 1996, A&A, 309, 633
Sellgren, K., Smith, R. G., & Brooke, T. Y. 1994, ApJ, 433, 179
Shalabiea, O. M., & Greenberg, J. M. 1994, A&A, 290, 266
Skinner, C. J., Tielens, A. G. G. M., Barlow, M. J., & Justtanont, K. 1992, ApJ, 399, L79
Smith, R. G., Sellgren, K., & Brooke, T. Y. 1993, MNRAS, 263, 749
Stapelfeldt, K. R., et al. 1995, ApJ, 449, 888
Sutton, E. C., Peng, R., Danchi, W. C., Jaminet, P. A., Sandell, G., & Russell, A. P. G. 1995, ApJS, 97, 455
Tamura, M., Nagata, T., Sato, S., & Tanaka, M. 1987, MNRAS, 224, 413
Tegler, S. C., Weintraub, D. A., Rettig, T. W., Pendleton, Y. J., Whittet, D. C. B., & Kulesa, C. A. 1995, ApJ, 439, 279
Tielens, A. G. G. M., Tokunaga, A. T., Geballe, T. R., & Baas, F. 1991, ApJ, 381, 181
Whittet, D. C. B., Adamson, A. J., Duley, W. W., Geballe, T. R., & McFadzean, A. D. 1989, MNRAS, 241, 707
Whittet, D. C. B., Adamson, A. J., McFadzean, A. D., Bode, M. F., & Longmore, A. J. 1988, MNRAS, 233, 321
Whittet, D. C. B., Duley, W. W., & Martin, P. G. 1990, MNRAS, 244, 427
Whittet, D. C. B., Smith, R. G., Adamson, A. J., Aitken, D. K., Chiar, J. E., Kerr, T. H., Roche, P. F., Smith, C. H., & Wright, C. M. 1996, ApJ, 458, 363
Willner, S. P., et al. 1982, ApJ, 253, 174